Journal of Electroceramics, 13, 605–608, 2004

Room Temperature Phase Transition in CeO_2 Nanocrystalline Films

ANNA KOSSOY,[1] JAYA P. NAIR,[1] ELLEN WACHTEL,[1] IGOR LUBOMIRSKY,*[1]
JUERGEN FLEIG[2] & JOACHIM MAIER[2]
[1]*Weizmann Institute of Science, Rehovot 76100, Israel*
[2]*Max Planck Institute for Solid State Research, Stuttgart, Germany*

Submitted February 3, 2003; Revised February 15, 2004; Accepted March 19, 2004

Abstract. The temporal evolution of the lattice parameter of oxygen deficient nanocrystalline cerium oxide films was monitored by X-ray diffraction. It was found that films with lattice parameter of ≈5.47 Å upon deposition undergo large spontaneous expansion, in which the size of the unit cell increases by ≈0.7% during the course of days. The films with as-deposited lattice parameter larger or smaller than ≈5.47 Å do not show significant changes. This behavior is consistent with the previously suggested hypothesis of an order-disorder transition of oxygen vacancies and can be viewed as its direct experimental confirmation.

Keywords: nanocrystalline ceramics, mechanical stress, diffusion, cerium oxide

Introduction

Development of miniature fuel cells capable of operating with different kinds of liquid or gaseous fuels is seen as a possible future alternative for batteries. The key element in such a fuel cell is a membrane of oxygen ion conductive material. Demands of small size and low operating temperature impose a limit of a few hundred nm on the thickness of the membrane. Therefore, nanocrystalline cerium dioxide based electrolytes are the prime candidates for the membrane material due to their high ionic conductivity and compatibility with silicon [1–4]. The last feature is especially important because it offers the possibility of fuel cells integrated with Si-based microelectromechanical systems (MEMS). Successful implementation of such systems depends on an understanding of mechanical stresses that, in the case of ion conductors, are linked to the oxygen content [5–8]. Thus chemical [9, 10] and mechanical properties of nanocrystalline CeO_2 are interdependent.

It has been reported recently [11] that membranes prepared from 1.5 μm thick nanocrystalline films of CeO_2 may expand by $\varepsilon = 1.4 \pm 0.6\%$ (Fig. 1) after substrate removal. On the basis of the X-ray and optical data the authors suggested [12] that the membranes that expanded contained two phases: fluorite CeO_{2-x} ($a = 5.4113$ Å [13]) and triclinic $Ce_{11}O_{20-y}$($a = 6.757$ Å, $b = 10.260$ Å, $c = 6.732$ Å, $\alpha = 90.04^\circ$, $\beta = 99.80^\circ$, $\gamma = 96.22^\circ$ [14, 15]). The latter can be viewed as a derivative of the fluorite phase with ordered oxygen vacancies and a pseudo-cubic lattice parameter of 5.47 Å. The partial specific volume of the triclinic phase is smaller than that of the fluorite phase and conversion of this phase into the fluorite phase should cause a linear expansion of 0.7%. Then the observed abnormally large lateral expansion of the membranes triggered by substrate removal could be attributed to the triclinic-to-fluorite phase transition. The authors complemented the optical and XRD data with a thermodynamic calculation which indicated that the strain at the film-substrate interface can completely suppress the phase transition. On the other hand, substrate removal may lead to a rapid phase transition [11, 16]. Although this hypothesis is consistent with all the experimental data, no direct evidence was presented regarding any change in the lattice parameter. One can expect that in nanocrystalline films, stress associated with substrate clamping will gradually relax. Hence, if the hypothesis

To whom all correspondence should be addressed. Email: Igor.Lubomirsky@weizmann.ac.il

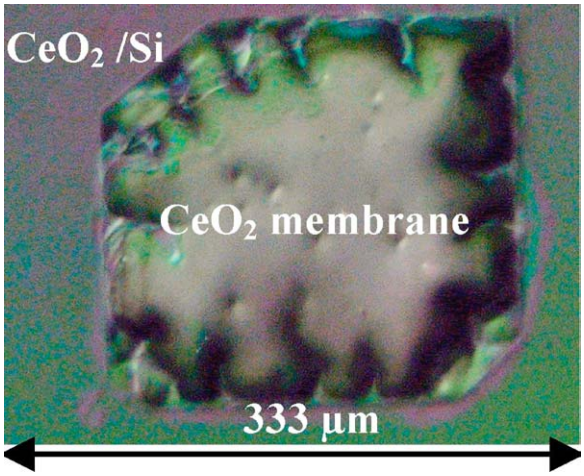

Fig. 1. Optical microscopy image (top view) of the expanded membrane. The height of the corrugation is 8–12 μm, corresponding to a lateral expansion of $\varepsilon = 1.4 \pm 0.6\%$. Due to the relatively small expansion the membrane adapts a single-dome shape, which is in agreement with ref. [22].

is correct, over a long period of time the phase transition must occur in substrate-supported films as well. The present study reports on real time observation of lattice changes in nanocrystalline CeO_2 films.

Experimental

Following ref. [11] RF sputtering was used to deposit 150 ± 30 nm thick cerium oxide films from a ceramic target of nominally undoped (99.95%) CeO_2 [17–19]. The deposition was performed at room temperature in pure Ar at 2×10^{-2} mBar pressure on Si wafer substrates. Without unloading the wafers from the vacuum chamber a 30 nm thick MgO encapsulation layer was deposited on top of the cerium oxide layer. The encapsulation layer was deposited by DC sputtering at 2×10^{-2} mBar of O_2 for 3 min and provided a pore-free barrier isolating the cerium oxide layer from the atmosphere. In a separate experiment it was verified that oxygen plasma oxidized CeO_2 after exposure of $\sim$1 hour. The grain size of the cerium oxide layer was determined by analyzing images obtained by scanning electron microscopy (SEM). A Dektak^3 surface profiler was employed to measure the thickness of cerium oxide and magnesium oxide layers. The bi-layer samples were kept at room temperature and the lattice parameter was monitored with a Rigaku D-max X-ray powder diffractometer (XRD) as a function of time.

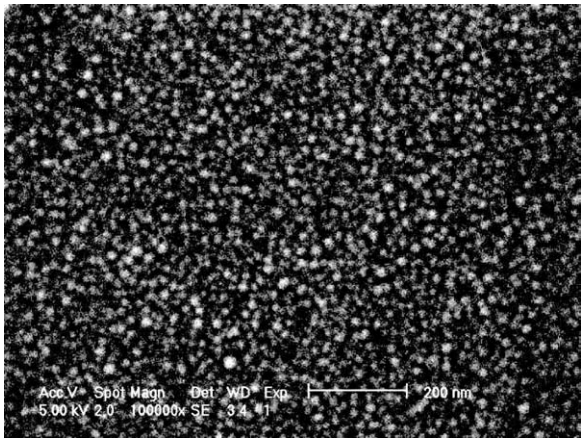

Fig. 2. SEM image of a cerium oxide film (without MgO capping layer) prepared by RF sputtering in pure Ar. The average grain size is 17 nm.

According to SEM (Fig. 2) the deposited films have a grain size of $\approx$17 nm. The XRD pattern of the films was consistent with that of CeO_2 and $Ce_{11}O_{20}$ cerium oxides [13, 15]. However, the close similarity of the XRD patterns of the fluorite (CeO_2) and triclinic phases ($Ce_{11}O_{20}$) did not allow differentiation between these phases. The (111) diffraction peak was the only one that could be monitored with an accuracy of $\pm$0.004 Å.

Results and Discussion

It has been found that as-prepared cerium oxide films have a pseudo-cubic lattice parameter of 5.45–5.53 Å depending on the deposition rate. For the samples ($N = 6$) with lattice parameter either significantly smaller or larger than 5.47 Å the lattice parameter was essentially unchanged with time. The samples that initially had a lattice parameter of 5.47 ± 0.1 Å ($N = 4$) showed a steady increase of the lattice parameter during the course of days. This process is usually accompanied by distortion of the shape of the (111) peak (Fig. 3) indicating that following the growth of the lattice parameter the (111) peak is a superposition of two closely spaced peaks. At the final stage (after $\approx$3 months) the lattice parameter approaches a value of 5.51 ± 0.1 Å (Fig. 4).

Since the radius of the Ce^{+3} ion is much larger than that of Ce^{+4}, oxidation of cerium oxide always causes a decrease in the size of the unit cell [20]. Thus the process occurring in the films could not possibly be an

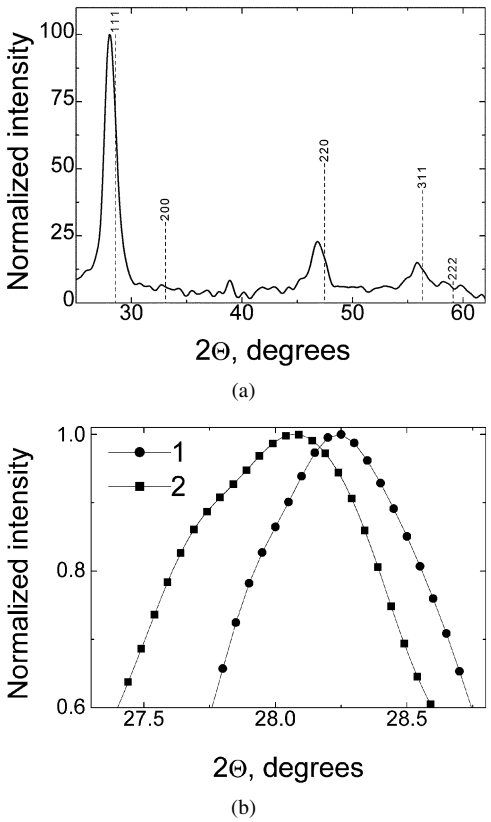

Fig. 3. (a) XRD spectrum of an as-deposited oxygen deficient cerium oxide film overlaid with the standard XRD spectrum of stoichiometric CeO_2 [13]. (b) The shape and position of the (111) peak in the XRD spectrum of the as-deposited film (1) and the same film after 84 days (2).

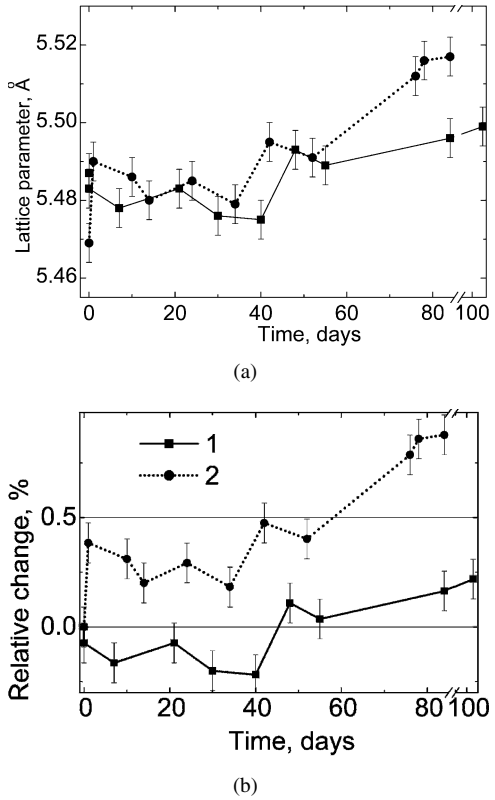

Fig. 4. (a) Shift in the position of the (111) peak for two samples of cerium oxide films covered by MgO capping layers. (b) Relative change of the lattice parameter with time. The sample prepared with the lattice parameter of 5.47 Å undergoes a large lateral expansion, whereas the sample prepared with lattice parameter > 5.48 Å remains practically unchanged. After ≈90 days no further changes in the lattice parameter were observed.

oxidation process. In addition the presence of the MgO capping layer prevents access of atmospheric oxygen to the cerium oxide layer. Thus an increase in the lattice parameter must be related to internal changes in the structure of cerium oxide. Measurable expansion of the lattice parameter is observed only if the initial value is close to 5.47 Å, which is the size of the pseudo-cubic cell of the triclinic phase $Ce_{11}O_{20}$. Furthermore, the increasing lattice parameter always stabilizes close to 5.51 Å, which is the unit cell dimension of an oxygen deficient fluorite structure with a stoichiometry of $CeO_{20/11}$.

The observed behavior can be explained as follows. According to the phase diagram constructed for the temperatures above 600 K [21] the fluorite phase and triclinic phase can coexist at 600–700 K and a single phase fluorite region is limited to a very narrow range of mean oxygen content $x = 0 - 0.02$ in CeO_{2-x}. This implies that the pseudo-cubic lattice parameter of any mixture of the fluorite phase and the triclinic phase must be within a range of 5.42 Å ($CeO_{1.98}$)–5.47 Å ($Ce_{11}O_{20}$). The pseudo-cubic lattice parameter above 5.47 Å should not exist because the next oxygen deficient phase Ce_7O_{12} has a distinctively different structure and XRD pattern. Experimentally observed XRD patterns correspond to a pseudo-cubic lattice parameter of 5.42–5.51 Å, which indicates that at room temperature the triclinic and the fluorite phases do not coexist, or coexist in a vary narrow range of mean oxygen content.

After deposition the films may have a phase composition different from the equilibrium composition for given mean oxygen content. If an as-deposited film contains predominantly the fluorite phase with or without a small amount of the triclinic phase, redistribution

of oxygen among the grains of the fluorite phase cannot cause significant changes in the mean lattice parameter. This is so because the size of the unit cell depends linearly on the oxygen content [20]. The lattice parameter for such samples can be anywhere between 5.4113 Å (stoichiometric CeO_2) to 5.52 Å (oxygen deficient fluorite $CeO_{20/11}$). If a film contains only the triclinic phase, then no further evolution is expected because atmospheric oxygen cannot penetrate through the MgO capping layer. If the major component of a film is the triclinic phase but the film contains also a significant amount of the fluorite phase, then oxygen diffusion from the fluorite phase may cause the oxygen content in the triclinic phase to increase above $CeO_{20/11}$. Once this happens a disordering of the oxygen vacancies will occur and the triclinic phase transforms into the fluorite phase, leading to a sharp increase of the lattice parameter from ≈5.47 Å (triclinic phase $Ce_{11}O_{20}$) to ≈5.51 Å (oxygen deficient fluorite $CeO_{20/11}$). Depending on the initial amount of the fluorite phase, the process continues till complete or partial transformation of the triclinic phase. In the latter case the film contains a mixture of two phases with the composition of each of them close to $CeO_{20/11}$, which agrees with the double-peak shape of the (111) XRD peak.

In conclusion, the data presented here are consistent with the previously suggested hypothesis [12] of an order-disorder transition of oxygen vacancies and can be viewed as a direct experimental confirmation. The experimental data also suggest that if there is a coexistence region of the fluorite and the triclinic phases at room temperature it must be very narrow.

Acknowledgments

The authors wish to acknowledge the Israel Ministry of Science, the Israeli Science Foundation and The German Federal Ministry of the Environment/Nature conservation and nuclear safety (BMU) for funding this research. I.L. is the incumbent of the Helen and Milton Kimmelman Career Development Chair.

References

1. H. Inaba and H. Tagawa, *Sol. State Ionics*, **83**, 1 (1996).
2. V.V. Kharton, F.M. Figueiredo, L. Navarro, et al., *J. Mater. Sci.*, **36**, 1105 (2001).
3. M. Hartmanova, K. Gmucova, and I. Thurzo, *Sol. State Ionics*, **130**, 105 (2000).
4. P. Tung Ming, C. Chao Hsin, L. Tan Fu, et al., *Electrochemical & Solid-State Letters*, **4**, F15 (2001).
5. A. Atkinson, *Sol. State Ionics*, **95**, 249 (1997).
6. A. Atkinson and T. Ramos, *Sol. State Ionics*, **129**, 259 (2000).
7. A. Atkinson and A. Selcuk, *Acta Materialia*, **47**, 867 (1999).
8. A. Atkinson and A. Selcuk, *Sol. State Ionics*, **134**, 59 (2000).
9. S. Kim and J. Maier, *J. Elecrochem. Soc.*, **149**, J73 (2002).
10. Y.M. Chiang, E.B. Lavik, I. Kosacki, et al., *J. Electroceram.*, **1**, 7 (1997).
11. Anomalous expansion of CeO_2 nanocrystalline membranes
12. J.P. Nair, E. Wachtel, I. Lubomirsky, J. Fleig, and J. Maier, *Adv. Mater* **15**, 2077 (2003).
13. Inorganic Crystal Structure Database, http://www.fiz-karlsruhe.de/fiz/products/icsd/icsd.html, ICSD Collection Code 72155
14. E.A. Kummerle and G. Heger, *J Solid State Chem.*, **147**, 485 (1999).
15. Inorganic Crystal Structure Database, http://www.fiz-karlsruhe.de/fiz/products/icsd/icsd.html, ICSD Collection Code 88758.
16. J.P. Nair, N. Stavitski, I. Zon, et al., *Europhys. Lett.* **60**, 782 (2002).
17. C.C. Chin, R.J. Lin, Y.C. Yu, et al., *Physica C*, **260**, 86 (1996).
18. M.S. Al-Robaee, K. Narasimha Rao, and S. Mohan, *J. Appl. Phys.*, **71**, 2380 (1992).
19. W. Lohwasser, J. Gerblinger, U. Lampe, et al., *J. Appl. Phys.*, **75**, 3991 (1994).
20. M. Mogensen, N.M. Sammes, and G.A. Tompsett, *Sol. State Ionics*, **129**, 63 (2000).
21. R. Korner, M. Ricken, J. Nolting, et al., *J Solid State Chem*, **78**, 136 (1989).
22. V. Ziebart, O. Paul, and H. Baltes, *J Microelectromech*, S **8**, 423 (1999).